

# Fermi Surface Properties of Low Concentration $\text{Ce}_x\text{La}_{1-x}\text{B}_6$ : dHvA.

A. A. Teklu,<sup>1</sup> R. G. Goodrich,<sup>1</sup> N. Harrison,<sup>2</sup> D. Hall,<sup>3</sup> Z. Fisk,<sup>3</sup> and D. Young<sup>3</sup>, <sup>1</sup> Department of Physics and Astronomy, Louisiana State University, Baton Rouge, LA 70803., <sup>2</sup> National High Magnetic Field Laboratory, LANL, MS-E536, Los Alamos, NM 87545., <sup>3</sup> National High Magnetic Field Laboratory, Florida State University, Tallahassee, FL 32310.

(March 20, 2000.)

The de Haas-van Alphen effect is used to study angular dependent extremal areas of the Fermi Surfaces (FS) and effective masses of  $\text{Ce}_x\text{La}_{1-x}\text{B}_6$  alloys for  $x$  between 0 and 0.05. The FS of these alloys was previously observed to be spin polarized at low Ce concentration ( $x = 0.05$ ). This work gives the details of the initial development of the topology and spin polarization of the FS from that of unpolarized metallic  $\text{LaB}_6$  to that of spin polarized heavy Fermion  $\text{CeB}_6$ .

## I. INTRODUCTION

The rare earth (RE) and divalent hexaborides have a variety of electrical, magnetic and thermodynamic properties and all have the same cubic structure. Among these materials are metallic  $\text{LaB}_6$  [1], Kondo insulating  $\text{SmB}_6$  [2], semi-metallic  $\text{CaB}_6$  [3 - 5], heavy Fermion (HF)  $\text{CeB}_6$  [6], and ferromagnetic  $\text{EuB}_6$  [7]. Extensive experimental and theoretical investigations have been done in order to understand their varying physical properties. One of the most decisive techniques to study the electronic properties of these materials is the de Haas - van Alphen (dHvA) effect with which the extremal cross-sectional areas of the Fermi surface (FS) and effective masses can be measured accurately. Pure  $\text{LaB}_6$  and pure  $\text{CeB}_6$  have been studied using this technique, having nearly identical prolate ellipsoidal FS's, with the FS of  $\text{CeB}_6$  being larger than that of  $\text{LaB}_6$  by about 10% [8,9]. For example, the values of the dHvA frequencies for  $\text{LaB}_6$  and  $\text{CeB}_6$  for the same minimum FS ellipsoid cross-section are 7.89 kT and 8.66 kT respectively. Yet, the effective masses are quite different being  $0.65m_e$  and  $30m_e$  (at 5-7 T) for  $\text{LaB}_6$  and  $\text{CeB}_6$  respectively [8,9], where  $m_e$  is the free electron mass.

There have been several electrical, magnetic and thermal studies carried out to explore how this transition from light metallic  $\text{LaB}_6$  to the HF  $\text{CeB}_6$  takes place when La ions are gradually replaced by Ce ions that introduce 4f electrons into the metal. In addition to this, experimental work has been carried out, using the dHvA effect at high magnetic fields ( $>20$  T), to explore the development of the HF behavior in  $\text{Ce}_x\text{La}_{1-x}\text{B}_6$  [10]. Here, it was reported that both the FS topology and effective masses transform continuously from that of pure  $\text{LaB}_6$  to that of pure  $\text{CeB}_6$  as the Ce concentration  $x$  is increased from 0 to 1. Furthermore, beginning at very low values of  $x$  (about 0.05), the contribution to the dHvA signal was observed to originate from only a single spin FS sheet.

Here we report detailed dHvA measurements, using both the field modulation technique at intermediate fields (6-15 T) and cantilever torque measurements to 30 T to investigate how the spin polarization manifests itself in the topological changes of the FS, and changes in effec-

tive masses of  $\text{Ce}_x\text{La}_{1-x}\text{B}_6$  alloys for  $0 \leq x \leq 0.05$ . The results of these measurements are then compared with the previous pulsed field measurements [10] and found to be in excellent agreement. In this paper, the spin polarization of the FS is investigated both qualitatively and quantitatively, and it is found that the spin up component dominates the dHvA signal as the Ce concentration increases.

## II. EXPERIMENT AND SAMPLE PREPARATION

Single crystals of  $\text{Ce}_x\text{La}_{1-x}\text{B}_6$  with  $x = 0, 0.01, 0.02, 0.03, 0.04$ , and 0.05 were grown in Al flux in the shape of rectangular parallelepipeds ( $1 \times 0.5 \times 2$  mm) with each face along a [100] axis of the cubic structure [11]. Most of the dHvA magnetization measurements on these samples were made in a 0-18 T superconducting magnet using the field modulation technique where a small time oscillating field  $h_0$  is superimposed on a steady state field. The sample was placed inside an astatic pair of pick up coils that was balanced to 1 part in  $10^4$  at zero field. The remaining imbalance signal voltage in the pick up pair due to the magnetization of the sample oscillating with changing magnetic field was detected using a lock-in amplifier.

Using field modulation, constant angle dHvA measurements were made in the field range 6-15 T with the field sweeping at a rate of 0.05 T/min and the field direction rotated within (100) crystal plane. From these dHvA oscillations one can determine the extremal cross-sectional areas and effective masses from the temperature dependence of signal amplitudes over the entire FS. The sample was further rotated continuously in a fixed field of 10 T to observe the detailed dependences of the FS cross sectional areas on angle. For these measurements, the sample rotator angle was calibrated so that the orientation of the sample was known to a precision of rotation of  $0.1^\circ$ . The above measurements were made at five or six different temperatures depending on the sample in the temperature range of 1.4 K to 4.2 K with the sample immersed in a pumped  $\text{He}^4$  bath. The sample temperature was mea-

sured using a calibrated Cernox thermometer and the vapor pressure of the bath. The field was calibrated with NMR.

To verify the reproducibility of these results, torque measurements on an  $x = 0.01$  Ce sample were made to 30 T at the National High Magnetic Field Laboratory, Tallahassee, FL.

### III. EXPERIMENTAL RESULTS

Figure 1 shows typical dHvA oscillations for  $\text{Ce}_x\text{La}_{1-x}\text{B}_6$  ( $x = 0.01$ ) for  $\theta = 0^\circ$  (i.e., the [100] direction) in the field range of 10–11 T and at a temperature of 1.4 K. A discrete Fourier transform (DFT) of the signal is shown on the same graph. For measurements on pure  $\text{LaB}_6$ , the frequency of the minimum area or  $\alpha_3$  orbit is found to be  $7.894 \pm 0.004$  kT, which is in good agreement with the original measurements of Arko et al.[1]. With this as a point of reference, complete angular dependent studies of the frequencies in all of the Ce concentrations were made. This study was made in order to check the assumption that the FS is represented by an ellipsoid of revolution, because this assumption had previously been used to calculate FS volumes [10]. Both constant angle field sweeps and constant field angle sweeps were obtained. Example data from the constant field rotation measurements for  $x = 0.01$  at  $T = 1.4$  K and  $H = 10$  T is shown in the inset of Figure 2. The oscillations with angle are caused by the fact that the dHvA phase,  $2\pi F(\theta)/H$ , changes by  $2\pi$  for each complete oscillation as  $\theta$  is varied. The angular variation of  $F$  can be determined from these rotation measurements using the counting method first implemented by Halse [12]. Using this technique, the angular variations of the minimum area or  $\alpha_3$  and maximum area or  $\alpha_{1,2}$  orbits were obtained. As a further check, field dependent measurements and DFTs were also made at several angles. An example of the complete data for  $x = 0.01$  is shown in Figure 2.

The effective masses of the different samples ( $0 \leq x \leq 0.05$ ) are extracted from the temperature dependences of the oscillation amplitudes. In comparison, the value of the effective mass of the  $\alpha_3$  orbit for  $x = 0$  or pure  $\text{LaB}_6$  was found to be  $0.66 \pm 0.03 m_e$  compared to the results of Arko et al. [1] which give  $0.65 m_e$ . Thus, the two values are the same to within experimental uncertainty.

### IV. DISCUSSION

It is well known that the cross-sectional area  $A$  of the FS in atomic units (a.u.) is related to the dHvA frequency  $F$  by the Onsager relation [13],

$$A(\text{a.u.}) = \left(\frac{2\pi e}{\hbar c}\right)F = 2.673 \times 10^{-5}F \quad (1)$$

where  $F$  is the dHvA frequency in tesla. From the measured values of the dHvA frequencies, the extremal cross-sectional areas of the  $\alpha_3$  and  $\alpha_{1,2}$  orbits for the field applied along the [100] crystal axis of Ce concentrations between  $x = 0$  and  $x = 0.05$  can be calculated. As shown in Figure 3, both of the frequencies corresponding to the  $\alpha_3$  and  $\alpha_{1,2}$  orbits are observed to increase with  $x$ . From these two frequencies, the volume of the FS, and hence the number of charge carriers per unit volume can be evaluated assuming that the FS is an ellipsoid of revolution. The  $x$  dependence of the carrier density,  $n$ , calculated in this manner is shown in the inset of Figure 3 [10].

It has been reported that both  $\text{LaB}_6$  and  $\text{CeB}_6$  have similar prolate electron ellipsoidal FS's situated at the six X points of the cubic Brillouin zone(BZ) that overlap along the  $\Gamma\text{R}$  symmetry axes [10,14]. This situation is shown schematically in Figure 4. The minimum cross-sectional area of the ellipse corresponding to the  $\alpha_3$ -orbit can be measured directly by applying the magnetic field  $\mathbf{H}$  along the [100] axis, while the maximum area for the  $\alpha_{1,2}$  orbit is only observed through magnetic breakdown (MB) for this same field orientation [10]. MB through the necks also leads to a multitude of frequencies  $\alpha_{1,2} + n\rho$  within the  $\Gamma\text{X}\text{M}$  plane,  $\rho$  being the orbit associated with a small FS orbit inside the necks and  $n$  is an integer [15]. The value of  $\rho$  is  $\sim 4 - 8$  T [16], which is smaller than our experimental uncertainty, and therefore cannot be resolved at the fields used for our measurements.

The expected angular dependence of the dHvA frequency from an ellipsoid of revolution is [17]:

$$\frac{1}{F(\theta)} = A \cos^2 \theta + B \sin^2 \theta + C \sin \theta \cos \theta \quad (2)$$

Here  $F(\theta)$  is the dHvA frequency and  $\theta$  is the angle of rotation from the principal axis of the ellipsoid normal to the field direction. A fit of the data to this equation is a useful criterion for deciding whether or not the FS is an ellipsoid of revolution [17]. We are interested here in the angular variations of the  $\alpha_3$  and  $\alpha_{1,2}$  orbits. If the [100] axis is rotated through an angle relative to the field direction in the (100) plane, the cross-sectional area of the FS normal to the field direction corresponding to the semi-minor axis of the ellipse, or the  $\alpha_3$  orbit, increases while the one corresponding to the semi-major axis or the  $\alpha_{1,2}$  orbit decreases, and these two areas or frequencies become degenerate at  $45^\circ$  (see Figure 2). These two frequencies and their fit to Equation 2 are plotted on the same graph in Figure 2, showing excellent agreement between the expected angular dependence from ellipsoidal FS and the data. This same agreement is obtained for all of the samples with  $0 \leq x \leq 0.05$  measured here. Thus, all of the measurements support the assumption used previously [9,10] that the FS is an ellipsoid of revolution.

Figure 5 shows the concentration ( $x$ ) dependence of  $m^*$  for the  $\alpha_3$  orbit and the curve fit to the data has the

quadratic form  $m_e(c + bx + ax^2)$ . According to Gor'kov and Kim, a linear dependence of the specific heat coefficient  $\gamma$  (proportional to  $m^*$ ) and the magnetic susceptibility  $\chi$  of Ce and U based alloys would be a signature of contributions from independent impurity centers [18]. However, at larger values of concentration in a system of localized spins, the linear dependence on  $x$  does not hold and Gor'kov and Kim [18] calculated an additional  $x^2$  correction term to both the specific heat and magnetic susceptibility, using the Fermi liquid formulation. Therefore, the very good fit of our data to a quadratic equation relating  $m^*$  and  $x$  would indicate that impurity centers are coupled even at low Ce concentrations. This observation is consistent with the model of coupled Ce atoms giving rise to the antiquadrupolar state in CeB<sub>6</sub> [19]. We would like to point out that the effective mass  $m^*$  could be spin-dependent. At this stage in the analysis, the effective mass  $m^*$  is the one determined from the temperature dependence of the dHvA signal which has contributions from spin up and spin down electrons. The spin dependence of  $m^*$  will be discussed later in Section V.

In the usual case when both spin states have the same mass, the magnetic field dependence of the dHvA amplitude can be used to determine the average Dingle temperature  $\bar{T}_D$  for the two spin states (see Section V). The effect of finite relaxation time due to impurity or point defects is to broaden the Landau levels leading to a reduction in amplitude roughly equivalent to that which would be caused by a rise of temperature to  $\bar{T}_D$ . The field dependence of the dHvA amplitude can be expressed as [17]

$$A_p = \frac{C_p T H^{-n} R_D}{\sinh(\alpha p T / H)} \quad (3)$$

where  $A_p$  is the amplitude of the  $p^{\text{th}}$  harmonic,  $R_D = \exp(-\alpha p \bar{T}_D / H)$  is the Dingle reduction factor,  $p$  is the harmonic number,  $\alpha = 14.69(m^*/m_e)T / K$ , and  $C_p$  and  $n$  depend on the particular method of measurement. For the torque method the value of  $n = -1/2$  and a plot of  $\ln(A_p H^{-1/2} \sinh(\alpha p T / H))$  versus  $1/H$  yields a straight line with a slope of  $\alpha p \bar{T}_D$  and a linear fit to the data gives  $m^* \bar{T}_D$ . A Dingle plot for the high field cantilever data for 1%Ce in LaB<sub>6</sub> at T=1.73 K and in the field range 10 – 25 T is given in Figure 6. From the slope of the straight line the value of the average Dingle temperature  $\bar{T}_D$  was found to be 3.5 K at high fields on the assumption that  $m = 0.73m_e$  for both spin states. We have analyzed the field dependence of the amplitude for all six samples ( $0 \leq x \leq 0.05$ ) using field modulation in the range  $7 \leq B \leq 15$  T and we found that  $m^* \bar{T}_D$  is the same within the measurement uncertainty. This means that the arbitrary substitution of La by Ce (or Ce by La) contributes little or nothing to the mean free path  $l$  of the dominant spin channel which is given by

$$\frac{l}{l_c} = \omega_c \tau \quad (4)$$

where  $l_c$  is the cyclotron length for a particular orbit given by [10]

$$l_c = \left( \frac{2\hbar F}{eB^2} \right)^{1/2}. \quad (5)$$

The average scattering rate is related to the average Dingle temperature by the relation

$$\bar{T}_D = \frac{\hbar}{2\pi k\tau}. \quad (6)$$

Thus, since  $m^* \bar{T}_D$  is independent of  $x$ , the mean free path  $l$  is also independent of  $x$  for a given field range. This observation is in agreement with the results of Goodrich et. al. [10] that the dominant source of scattering should originate from other forms of crystallographic imperfections not from the Ce or La impurities.

## V. SPIN DEPENDENT SCATTERING (SDS)

One of the effects of an applied magnetic field is to lift the spin degeneracy of the energy levels and the contributions to the dHvA signal from the spin-up and spin-down electrons. In conventional metals, the effect of the Zeeman splitting is to reduce the amplitude by a spin reduction factor  $R_S$  given by[17]

$$R_S = \cos\left(\frac{1}{2}p\pi g \frac{m^*}{m_e}\right) \equiv \cos(p\pi S) \quad (7)$$

where  $g$  is the spin-splitting factor and  $m_e$  is the free electron mass. We had reported earlier that above 5% Ce in LaB<sub>6</sub>, the contribution to the dHvA amplitude originates from a single spin FS. One explanation of this observation is that scattering from spin fluctuations does not occur with equal strength for the two spin directions. There is a large negative magnetoresistance [20] in Ce<sub>x</sub>La<sub>1-x</sub>B<sub>6</sub> alloys that can be explained by the suppression of spin fluctuation scattering. However, from magnetoresistance measurements one cannot determine if one or two spin states are contributing to the scattering. Part of the purpose of the present work was to study in detail how the single spin dHvA signal develops in CeB<sub>6</sub> from the two spin signal in pure LaB<sub>6</sub>.

In the presence of high magnetic fields, if there is only one spin contribution to the signal, then a plot of  $\ln(A_p / p^{1/2})$  against the harmonic number,  $p$ , yields a straight line because the spin splitting reduction factor as is given by Equation 7 is no longer present. However, if there are contributions to the dHvA amplitude from spin-up and spin-down states, there is spin reduction of the amplitude and we observe non linear dependence of  $\ln(A_p / p^{1/2})$  on  $p$  as shown in Figure 7 for  $0 \leq x \leq 0.05$  except for  $x \geq 0.05$ , the concentration at which only one spin component is observed.

For pure LaB<sub>6</sub>, the dHvA amplitudes associated with the spin-up and spin-down electrons are equal. However,

if magnetic impurities are involved, we could expect spin dependent scattering and the amplitudes for spin-up and spin-down oscillations could be unequal corresponding to unequal Dingle temperatures. So, the signal amplitude measured with the field modulation technique, which has contributions from both the spin-up and spin-down components, has to be modified in order to account for differences in Dingle temperatures and masses between the two spin channels. In the first harmonic detection, this signal voltage is related to the oscillatory magnetization by [21]

$$\tilde{V}(\zeta) = G \sum_p \tilde{M}_p J_1(p\Lambda) \sin(p\zeta + \theta_p), \quad (8)$$

where  $G$  represents the system gain,  $\tilde{M}_p$  is the magnetization due to the  $p^{\text{th}}$  harmonic of the dHvA signal,  $J_1$  is a Bessel function of order one,  $\Lambda = 2\pi h/H^2$ ,  $h$  is the modulation amplitude,  $\zeta = 2\pi F/H$ ,  $\sigma = \pm 1$ , and  $\theta_p$  is the phase. The magnetization  $\tilde{M}$  can be written [21]:

$$\tilde{M} = \sum_{p=1}^{\infty} \sum_{\sigma} C_p D^p E^{\sigma p} \sin(p\zeta + p\frac{\pi}{4} - \sigma p\pi S) \quad (9)$$

where

$$D = \exp(-K m^* \bar{T}_D / H), \quad (10)$$

$$\bar{T}_D = (T_D^{\downarrow} + T_D^{\uparrow})/2 \quad (11)$$

$$E = \exp(-K m^* (\delta T_D) / H) \quad (12)$$

$$\delta T_D = (T_D^{\downarrow} - T_D^{\uparrow})/2 \quad (13)$$

and

$$C_p = \frac{\nu T F}{(A'' p \hbar)^{1/2}} \frac{1}{\sinh(p K m^* T / H)} \quad (14)$$

where  $\nu = 1.304 \times 10^{-5} (Oe^{1/2}/K)$ ,  $K = 14.69(T/K)$ ,  $F$  is the dHvA frequency and  $A$  is the extremal cross sectional area of the FS.

If the phase difference  $\phi_p (= p\pi S)$  between spin-up and spin-down oscillations is field dependent, the first two harmonics of the magnetization  $\tilde{M}$  may also be written as

$$\tilde{M}_1 = C_1 \left[ z \sin(\psi + \frac{\phi}{2}) + z' \sin(\psi - \frac{\phi}{2}) \right] \quad (15)$$

$$= C_1 (z^2 + z'^2 + 2zz' \cos \phi)^{1/2} \sin(\psi + \theta_1) \quad (16)$$

and

$$\tilde{M}_2 = C_2 (z^4 + z'^4 + 2z^2 z'^2 \cos(2\phi))^{1/2} \sin(2\psi \mp \frac{\pi}{4} + \theta_2) \quad (17)$$

where  $z$  is the Dingle reduction factor for the spin up electrons,  $z'$  is the Dingle reduction factor for the spin down electrons, and  $\psi$  is defined to be  $(2\pi F/H) \pm \pi/4$

where the upper sign is for a minimum FS area and the lower is for a maximum FS area. Other higher harmonics can be written in a similar way. The relative phase between the spin up and down components of the signal is given by

$$\tan \theta p = \frac{z^p - z'^p}{z^p + z'^p} \tan(\frac{p\phi}{2}) \quad (18)$$

and the spin up and the spin down Dingle reduction factors for the  $p^{\text{th}}$  harmonic are given by

$$z^p = \exp(-p\alpha T_D^{\uparrow} / H) \quad (19)$$

and

$$z'^p = \exp(-p\alpha T_D^{\downarrow} / H) \quad (20)$$

The relative phases are obtained by fitting the data to the first three harmonics of the magnetization. From the measured signal harmonic amplitude ratios  $M_2/M_1$ ,  $M_3/M_1$  and the relative phases between the harmonics  $(\theta_2 - 2\theta_1)$  and  $(\theta_3 - 3\theta_1)$ , we calculate, at a given  $H$  and  $T$ , the values of the amplitudes  $D$  and  $E$  (i.e.,  $m^* \bar{T}_D$  and  $m^* \delta T_D$ ), and the value of  $S$ . Once the value of  $S$  is known, we can determine the amplitude ratio  $z'/z$  (or  $(m^{\downarrow} T_D^{\downarrow} - m^{\uparrow} T_D^{\uparrow})$ ). The average Dingle temperature,  $\bar{T}_D$ , is spin independent while the difference  $\delta T_D = (T_D^{\uparrow} - T_D^{\downarrow})/2$  shows the spin-dependence. As mentioned earlier, the effective mass  $m^*$  could also depend on spin. Therefore, since in all of the above expressions the product  $m^* T_D$  where both  $m^*$  and  $T_D$  are spin-dependent always occurs, it is not trivial to single out the spin dependence of either one. Therefore, we will first assume that  $m^{\uparrow} = m^{\downarrow}$  so that  $C_p$  (Eqn. 14) is the same for both spin states. The concentration dependence of  $m(T_D^{\downarrow} - T_D^{\uparrow})$  is then calculated from the amplitude ratios  $M_2/M_1$ ,  $M_3/M_1$  and relative phases. Next, we assume  $m^{\uparrow} \neq m^{\downarrow}$  such that  $C_p^{\downarrow} \neq C_p^{\uparrow}$  and again calculate the  $x$  dependence, now of  $(m^{\downarrow} T_D^{\downarrow} - m^{\uparrow} T_D^{\uparrow})$ . Figure 8 shows the concentration dependence of both  $m(T_D^{\downarrow} - T_D^{\uparrow})$  and  $(m^{\downarrow} T_D^{\downarrow} - m^{\uparrow} T_D^{\uparrow})$  and there is clear evidence of SDS. In other words, if there is no SDS, then  $\delta T_D = T_D^{\downarrow} - T_D^{\uparrow} = 0$ , that is the slope of the  $x$  dependence of  $(m^{\downarrow} T_D^{\downarrow} - m^{\uparrow} T_D^{\uparrow})$  is non-zero. The circles represent the case that  $m^{\uparrow} = m^{\downarrow}$ , while the squares represent the case  $m^{\uparrow} \neq m^{\downarrow}$ . The slope of the line corresponding to  $m^{\uparrow} \neq m^{\downarrow}$  is approximately eight times that corresponding to  $m^{\uparrow} = m^{\downarrow}$  indicating that  $m^{\downarrow} T_D^{\downarrow}$  becomes greater than  $m^{\uparrow} T_D^{\uparrow}$  as the Ce concentration increases, that additional increase in slope arising from the difference in mass.

For  $\text{LaB}_6$ , the two spin components have equal amplitudes and the amplitude ratio  $z'/z$  is equal to one or  $\delta T_D = T_D^{\downarrow} - T_D^{\uparrow} = 0$ . In other words, the scattering rates for spin up and spin down are equal. As the Ce concentration is increased to 5%, the ratio of the spin-up to the spin-down amplitude increases confirming the complete

observed spin polarization of the FS at 5%Ce in  $\text{LaB}_6$  to one spin channel which is the spin up.

There are two contrasting theories concerning whether the FS polarizes to the spin up or spin down state. The first is the theory developed by Wasserman et al. [22] for quantum oscillations in heavy fermion materials. This model, along with its zero field predecessor [23], is successful in accounting for the heavy effective masses as well as small topological changes in the FS caused by the presence of additional f electrons. However, this model also predicts that the dHvA signal is dominated by the spin down channel, and that its associated effective mass should decrease in a magnetic field. While apparent evidence for this was reported in very heavy compounds such as  $\text{CeCu}_6$  [24], it is  $\text{CeB}_6$  that shows perhaps the most dramatic mass changes with increasing magnetic field [25], but the polarity of the spin was not identified.

A large number of measurements have been performed on  $\text{CeB}_6$  [26-34], which is regarded as a typical dense Kondo lattice with a very low Kondo temperature of 1–2 K. Previous experimental data have appeared to be entirely consistent with the theoretical model of Wasserman et al. [22], that is, the effective mass is dramatically suppressed in a magnetic field [25]. Recent measurements [9] have shown that in addition to the suppression of the effective mass, there is notable deformation in the topology of the FS in a magnetic field, and this result is not entirely consistent with the mean field theory of Ref. [22]. One aspect of the result that does appear to be consistent with this theoretical model, though, is that the dHvA signal originates from only a single spin FS sheet [9], even though the theory must be fundamentally incorrect because it predicts the wrong spin state to be observed.

All of the dHvA measurements on  $\text{CeB}_6$  are made in the high magnetic field regime well above the metamagnetic transition where the dipole moments of the f electrons are essentially aligned. According to Edwards and Green [35], in this regime the theory developed by Wasserman et al. [22] is no longer applicable. This is due to the fact that this is a mean field approach in which the interactions are assumed not to change in a magnetic field. Making such a description of the dHvA effect in HF systems is really only valid at low magnetic fields, that is, magnetic fields less than the Kondo temperature scale. Edwards and Green [35] instead make the analogy of a HF compound in a magnetic field to a itinerant ferromagnet, in which spin fluctuations play a decisive role. Edwards and Green [35] also anticipate that the dHvA effect should be dominated by only a single spin, but the up spin instead of the down spin. Therefore, one can see that our measurements are in agreement with the predictions of Edwards and Green that the down spin mass enhancement is larger than that of the up spin and does not contribute to the dHvA signal amplitude.

As further verification of this mass difference, we use Equations (19) and (20) to write

$$-\frac{H}{K} \ln(z/z') = (m^\downarrow - m^\uparrow)T + (m^\downarrow T_D^\downarrow - m^\uparrow T_D^\uparrow) \quad (21)$$

The quantity on the left hand side of Equation 21 is calculated for each value of  $x$  and plotted versus  $T$  in Figure 9. It can be seen that the data is linear in  $T$  with a slope of  $(m^\downarrow - m^\uparrow)$  and intercept  $(m^\downarrow T_D^\downarrow - m^\uparrow T_D^\uparrow)$ . The value of  $(m^\downarrow - m^\uparrow)$  ranges from 0.003 for  $x = 0$  or pure  $\text{LaB}_6$  to 0.09 for  $x = 0.05$  respectively. In addition, the value of  $(m^\downarrow T_D^\downarrow - m^\uparrow T_D^\uparrow)$  ranges from 0.03 for  $x = 0$  to 0.3 for  $x = 0.05$ . Thus, for pure  $\text{LaB}_6$ , which is not spin polarized,  $m^\downarrow = m^\uparrow$  as expected. As the Ce concentration increases to 5%,  $(m^\downarrow - m^\uparrow)$  increases with  $m^\downarrow$  being greater than  $m^\uparrow$  by about 10%. If this mass difference continues to increase with  $x$  the observed discrepancy between specific heat and dHvA mass measurements in  $\text{CeB}_6$  is explained. Moreover, the difference in the scattering parameter,  $(m^\downarrow T_D^\downarrow - m^\uparrow T_D^\uparrow)$ , increases with the Ce concentration confirming that the observed FS is due only to the spin up state. These observations lead us to the conclusion that it is the combination of  $\Delta m^*$  and SDS that takes the down spin out of the dHvA signal. Therefore, both  $\Delta m^*$  and SDS are equally important in understanding many of the properties of  $\text{CeB}_6$ .

## VI. CONCLUSION

We have performed a detailed microscopic dHvA study of low concentration (up to  $x = 0.05$ ) in  $\text{Ce}_x\text{La}_{1-x}\text{B}_6$  alloys and determined the development of the size and geometry of the FS from that of spin unpolarized  $\text{LaB}_6$  to the spin polarized  $\text{Ce}_x\text{La}_{1-x}\text{B}_6$  ( $x \geq 0.05$ ) alloys. We have shown:

- The spin up signal amplitude dominates the dHvA signal when the Ce concentration is  $\geq 5\%$ .
- We determined that the down spin mass is greater than that of the up spin and the spin down contribution to the dHvA signal amplitude is small.
- The angular dependence of the dHvA extremal areas of the FS show that the assumption that the FS is an ellipsoid of revolution is valid for all concentrations measured.
- The dependence of the effective mass on concentration is in agreement with the existing theories of magnetic impurity interactions [18].

Overall, this work is the most detailed study using dHvA of alloy systems involving magnetic ions with concentrations greater than 1% that has been reported.

### Acknowledgment

A portion of this work was performed at the National High Magnetic Laboratory, which is supported by NSF Cooperative agreement No. DMR - 9527035 and by the State of Florida. Additional support from the NSF (DMR9971348) is acknowledged by Z. Fisk.

## References

1. A. P. J. Arko, et al., *Phys. Rev. B* **13**, 5240 (1976)
2. P. Nyhus, et al., *Phys. Rev. B* **55**, 12488-12496 (1997)
3. H. C. Longuet-Higgins and M. de V. Roberts, *Proc. Roy. Soc. London A* **224**, 336-347 (1954)
4. W. A. C. Erkelens, et al., *J. Magn. Magn. Mater.* **63/64**, 61-63 (1987)
5. D. P. Young, et al., *Nature* **397**, 412 (1999)
6. S. Sullow, et al., *Phys. Rev. B* **57**, 5860-5869 (1998)
7. L. Degiorgi, et al., *Phys. Rev. Lett.* **79**, 5134-5137 (1997)
8. A. P. J. van Deursen, Z. Fisk and A. R. de Vroomen, *Solid State Commun.* **44**, 609 (1982)
9. N. Harrison, et al., *Phys. Rev. Lett.* **81**, 870 (1998)
10. R. G. Goodrich, et al., *Phys. Rev. Lett.* **82**, 3669 (1999)
11. R. G. Goodrich, et al., *Phys. Rev. B* **58**, 14896 (1998)
12. M. R. Halse, *Phil. Trans. Roy. Soc. A* **265**, 53 (1969)
13. L. Onsager, *Phil. Mag.* **43**, 1006 (1952)
14. Y. Onuki, et al., *J. Phys. Soc. Jpn.* **58**, 3698 (1989)
15. N. Harrison, et al., *Phys. Rev. Lett.* **80**, 4498 (1998)
16. Y. Ishizawa, et al., *J. Phys. Soc. Jpn.* **48**, 1439 (1980)
17. D. Shoenberg, *Magnetic Oscillations in Metals* (Cambridge University Press, Cambridge, 1984)
18. L. P. K. Gor'kov and Ju H. Kim, *Phys. Rev. B* **51**, 3970 (1995)
19. F. J. Ohkawa, *J. Phys. Soc. Japan* **52**, 3897 (1983)
20. N. Sato, et al., *J. Phys. Soc. Jpn.* **54**, 1923 (1985)
21. Alles, H. G., Higgins, R. J. and Lowndes, D. H. *Phys. Rev. Lett.* **30**, 705 (1973)
22. A. Wasserman, M. Springford, and F. Han, *J. Phys.: Condens. Matter* **3**, 5335 (1991)
23. J. W. Rasul, *Phys. Rev. B* **39**, 663 (1989)
24. S. B. Chapman, et al., *Physics Lett. B* **163**, 361 (1990)
25. N. Harrison, et al., *J. Phys.: Condens. Matter* **5**, 7435 (1993)
26. A. P. J. van Deursen et al., *J. Less-Common Mat.* **111**, 331 (1985)
27. W. Joss, et al., *Phys. Rev. Lett.* **59**, 1609 (1987)
28. R. Foro, et al., *J. Phys. Soc. Jpn.* **57**, 2885 (1988)
29. W. Joss, et al., *de Physique* **49**, 747 (1988)
30. W. Joss, *J. Mag. and Mag. Mat.* **84**, 264 (1990)
31. Y. Onuki, et al., *Physica B* **163**, 100 (1990)
32. E.G. Haanappel, et al., *Physica B* **177**, 181 (1992)
33. H. Matsui, et al., *Physica B* **186-188**, 126 (1993)
34. R. Hill et al., *Physica B* **230-232**, 114 (1997)
35. D. M. Edwards and A. C. Green, *Z. Phys. B* **103**, 243 (1997).

## FIGURE CAPTIONS

FIG. 1 An example of dHvA oscillations from the field modulation measurements for  $x = 0.01$  sample for H along the [100] axis. The inset shows the DFT of the oscillations for a field range of 10 – 11 T.

FIG. 2 The dHvA frequencies  $F_3$  and  $F_{1,2}$  as a function of orientation for  $x = 0.01$  from field sweep and rotation (high density points in the Fig.) measurements. The solid lines are the fits to the ellipsoid Eqn. 2. The inset shows the raw data from angular sweep measurements at 10 T.

FIG. 3 Ce concentration dependence of the dHvA frequencies  $F_3$  and  $F_{1,2}$  at fields 10 – 11 T. The inset shows the number of electrons per unit volume,  $n$ , as a function of  $x$ .

FIG. 4 FS of  $\text{LaB}_6$ .

FIG. 5 The Ce concentration dependence of cyclotron mass for the  $\alpha_3$  orbit at 10 T. The solid line is a quadratic fit to the data.

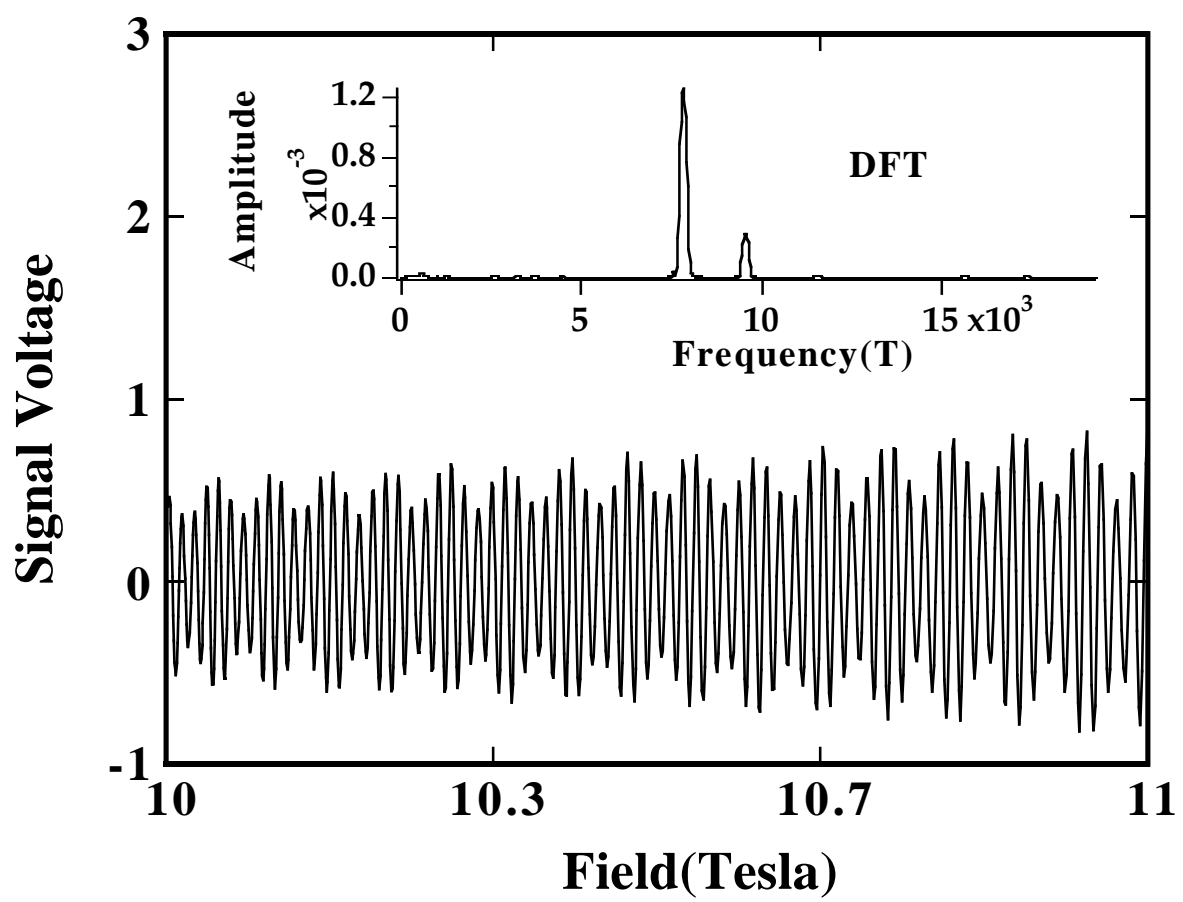
FIG. 6 Dingle plot for  $x = 0.01$  at 1.73 K in the field range of 10 – 25 T using the cantilever technique.

FIG. 7 A plot of  $\ln(A_p / p^{1/2})$  versus the harmonic number  $p$  for  $x = 0$  to 0.05. Note that it becomes linear at  $x = 0.05$ .

FIG. 8 Ce concentration dependence of  $m^\downarrow T_D^\downarrow - m^\uparrow T_D^\uparrow$ .

FIG. 9 Temperature dependence of  $(H/K) \ln(z/z')$  for all the alloys including pure  $\text{LaB}_6$ . From the linear fits to the data, mass differences between the two spin states were determined.

**Fig. 1 of Teklu et. al.**



**Fig. 2 of Teklu et. al.**

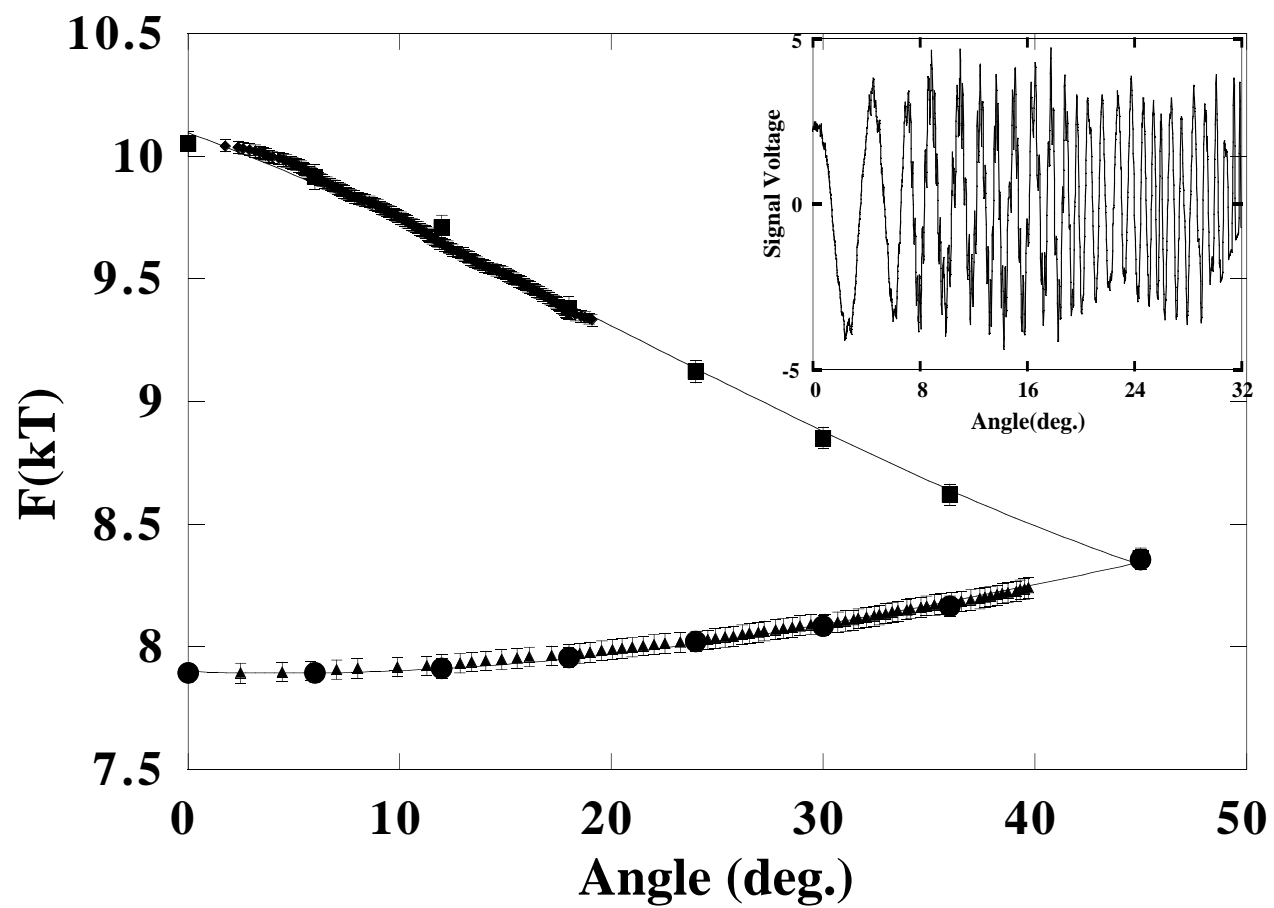
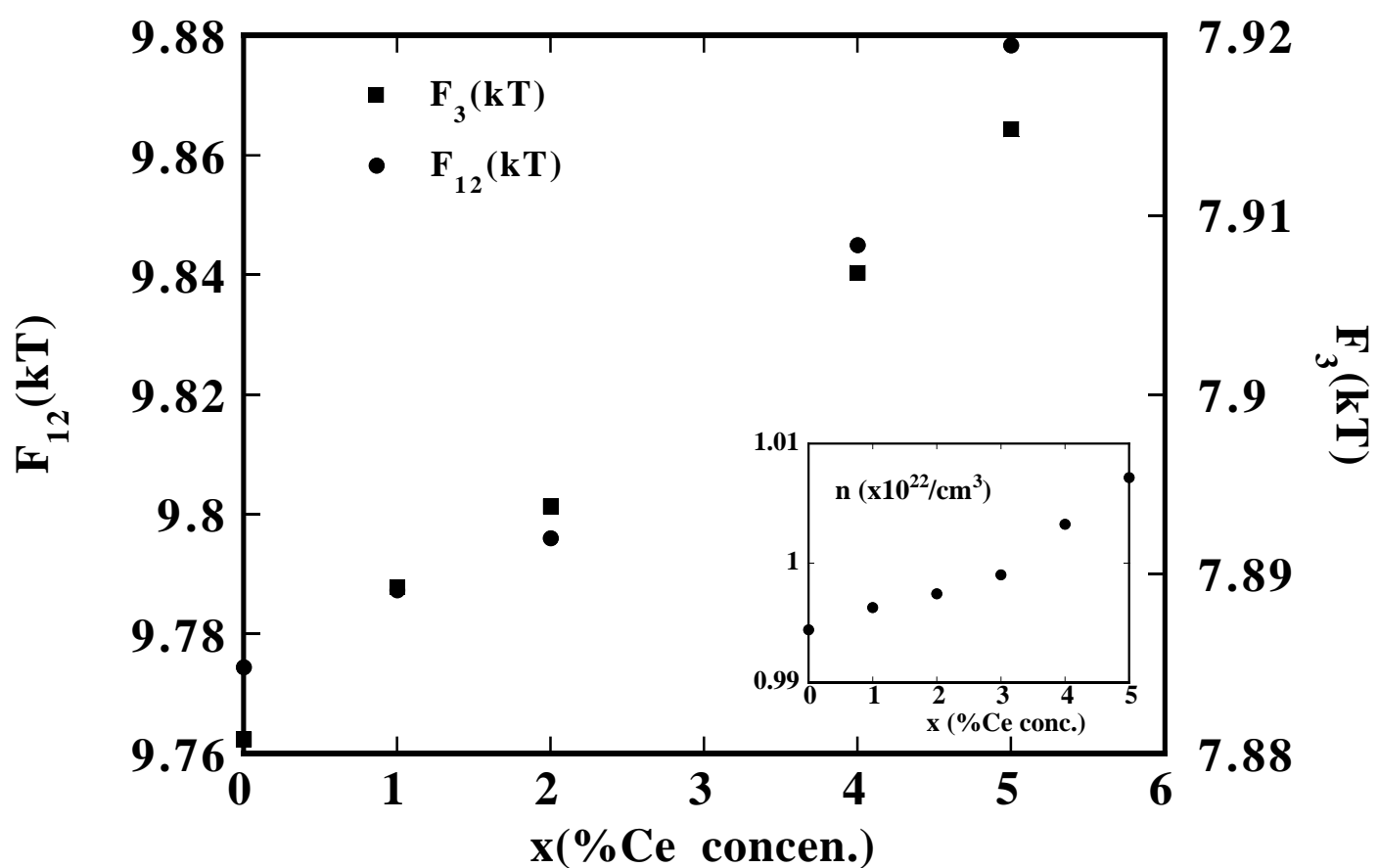


Fig. 3 of Teklu et. al.



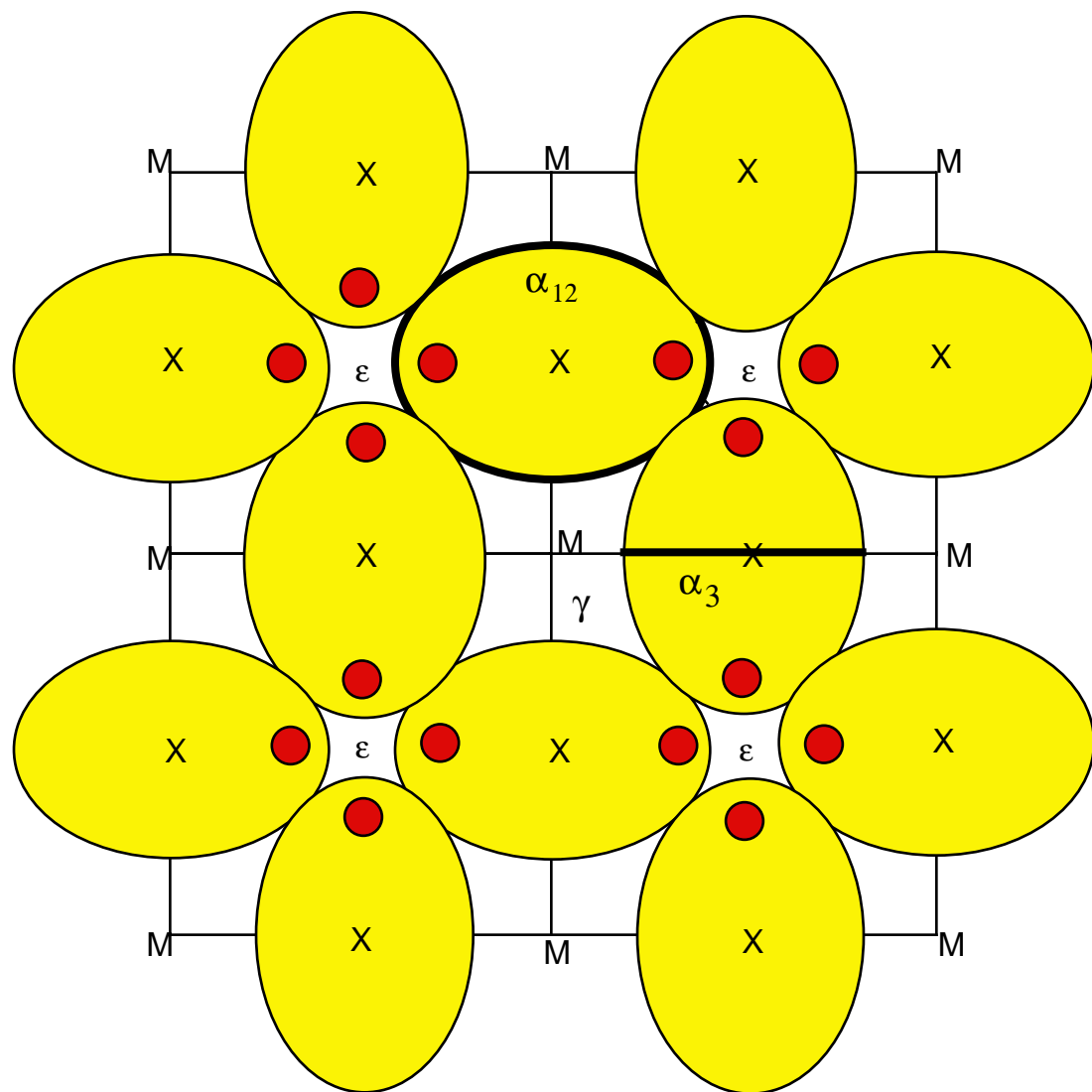
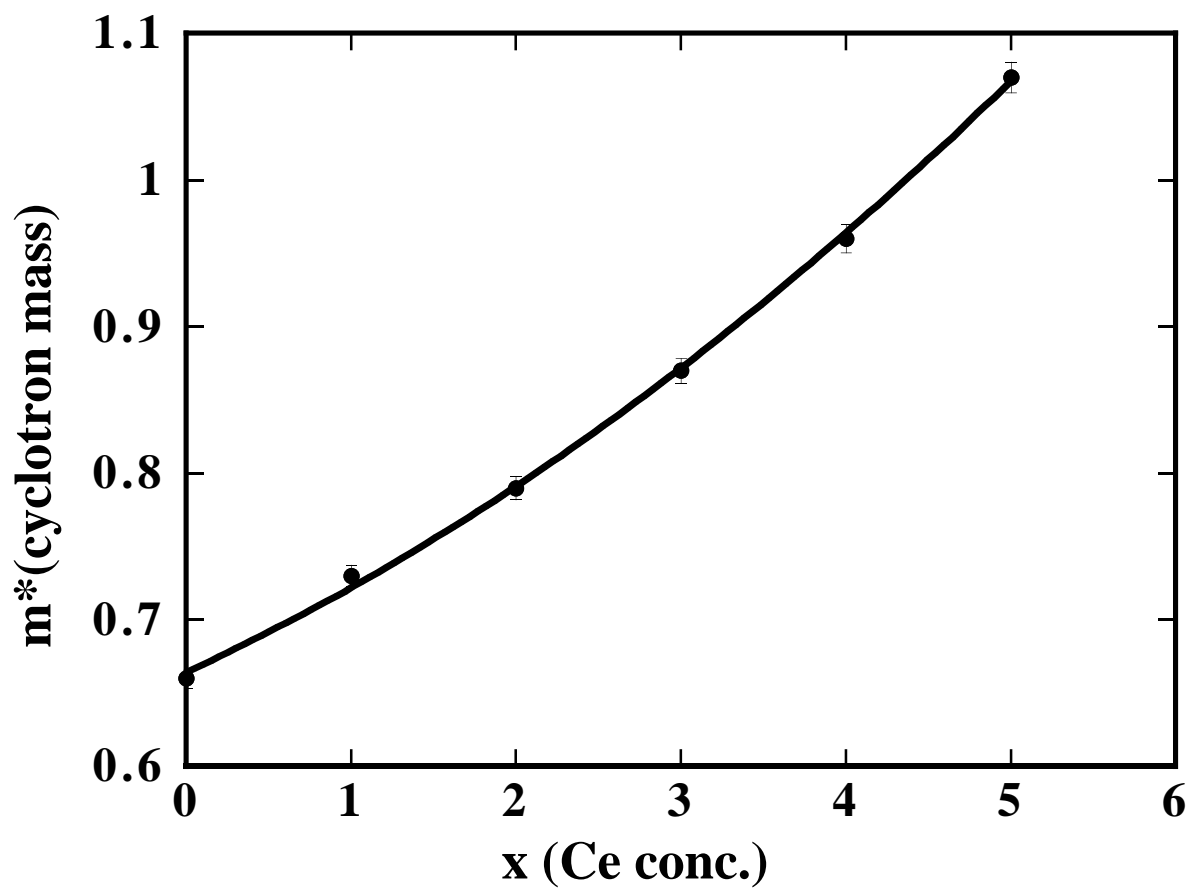
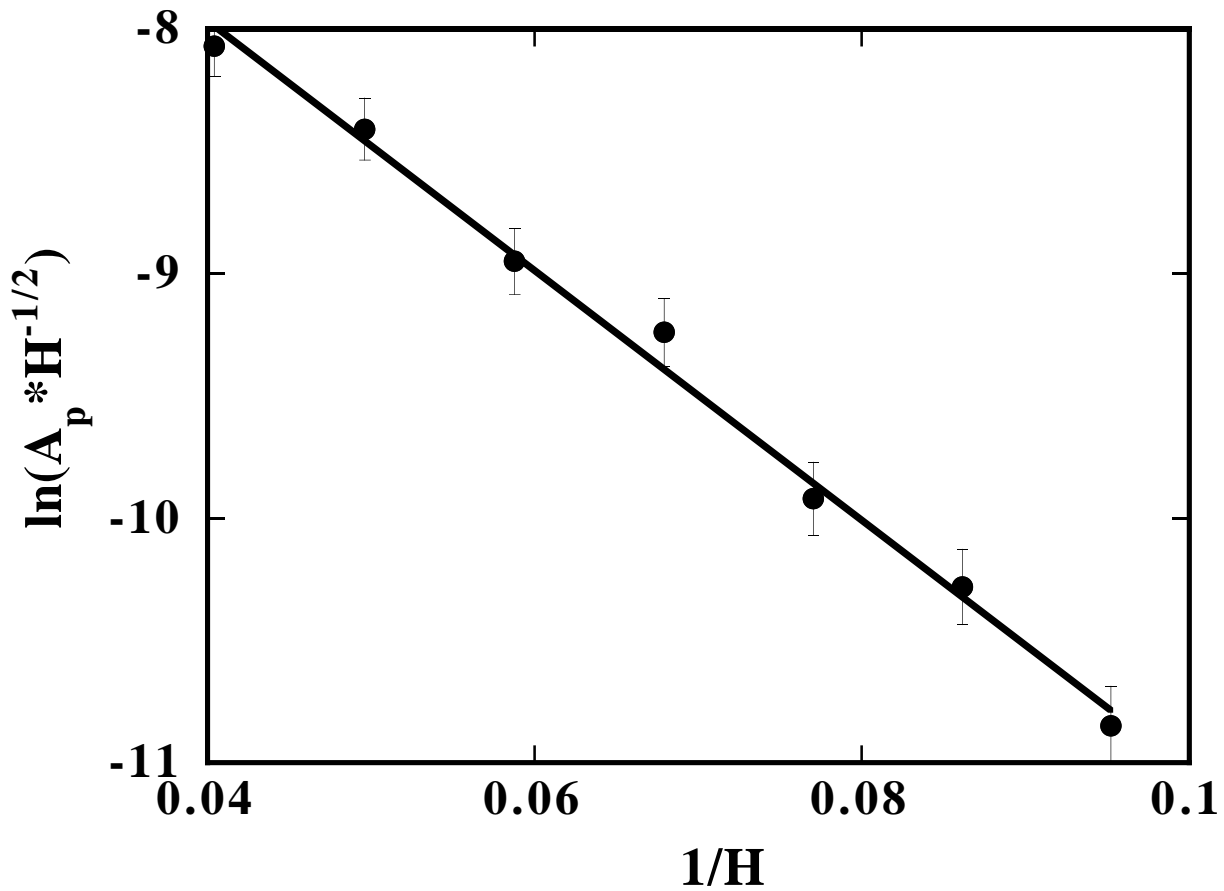


Fig. 4 of Teklu et al

**Fig. 5 of Teklu et. al.**



**Fig. 6 of Teklu et. al.**



**Fig. 7 of Teklu et. al.**

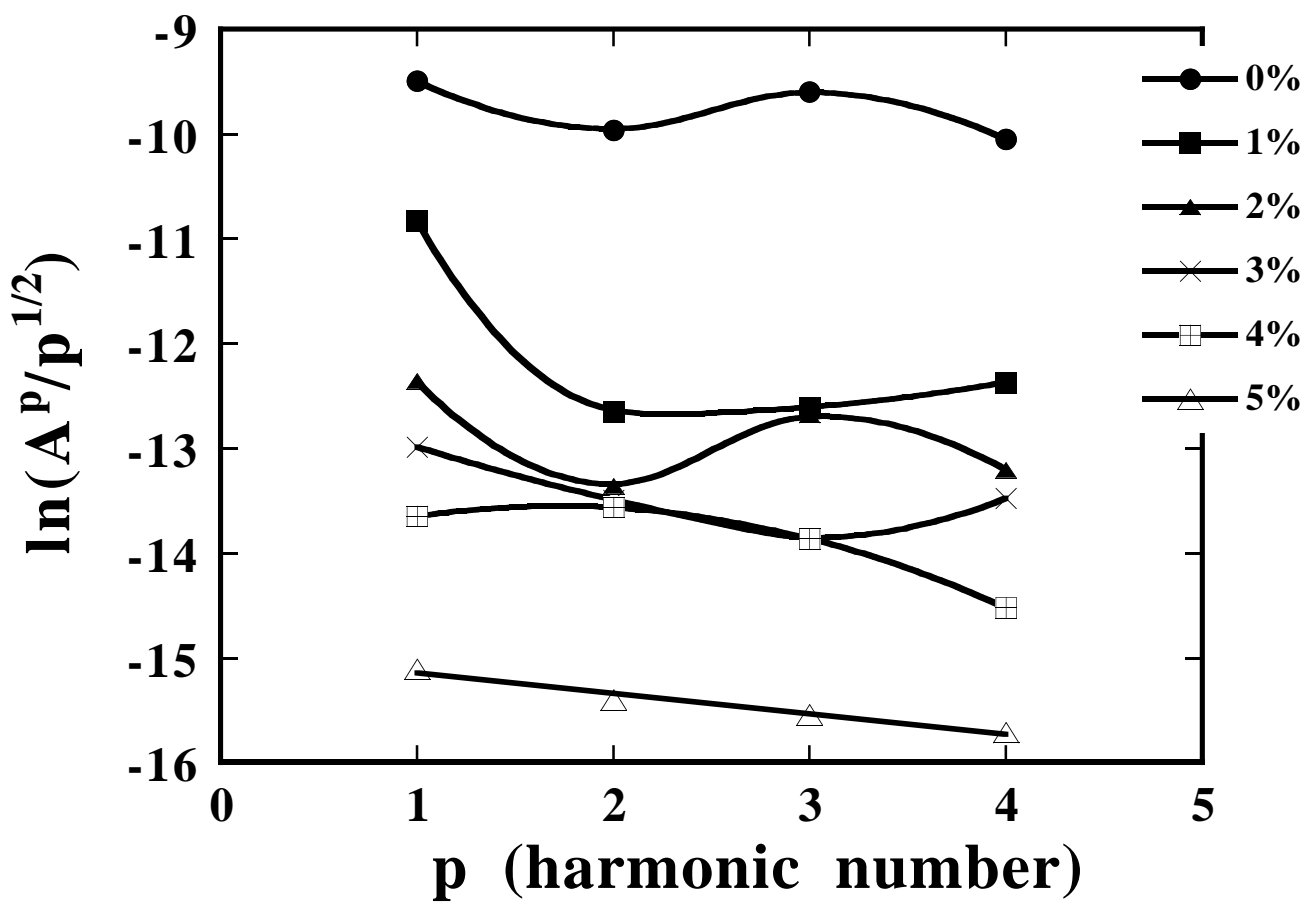


**Fig. 8 of Teklu et. al.**

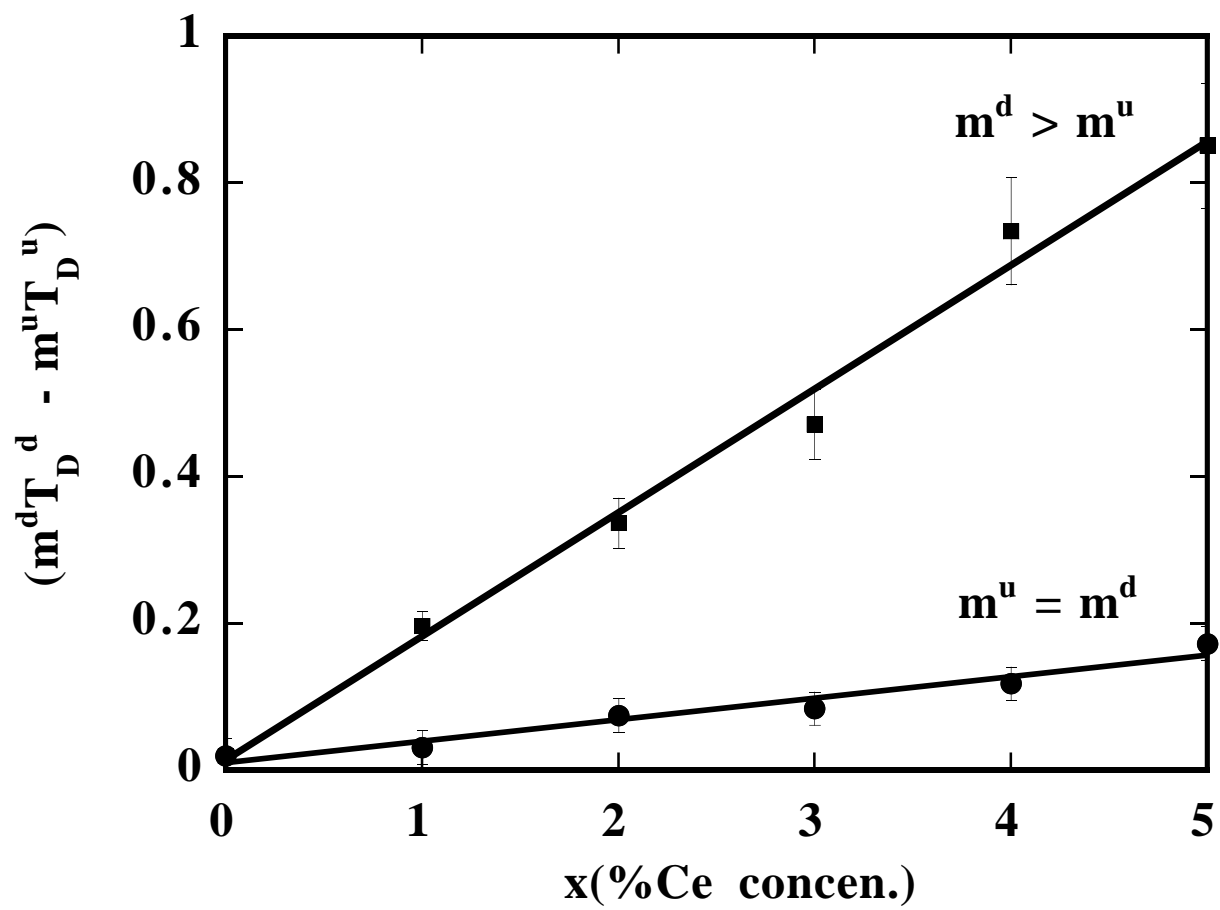


**Fig. 9 of Teklu et. al.**

